Supplemental Information for:

Single-cell multi-omics reveals dynamic chromatin remodeling of adaptive immunity during prime-boost vaccination

Rong Wang [1,2,†], Huajie Hu [1,2,†], Xuan Li [1,2], Zijie Scott Zhang [1,2,3,*] Rui Cheng [1,2,*]

[1] Bio-X Center for Interdisciplinary Innovation, Yunnan University, Kunming, 650091, China
[2] Yunnan Vaccine Laboratory, Kunming, 650091, China
[3] Southwest United Graduate School, Kunming, Yunnan 650092, China.

Correspondence to:
Zijie Scott Zhang, zijiezhang@ynu.edu.cn;
Rui Cheng, ruicheng@ynu.edu.cn;

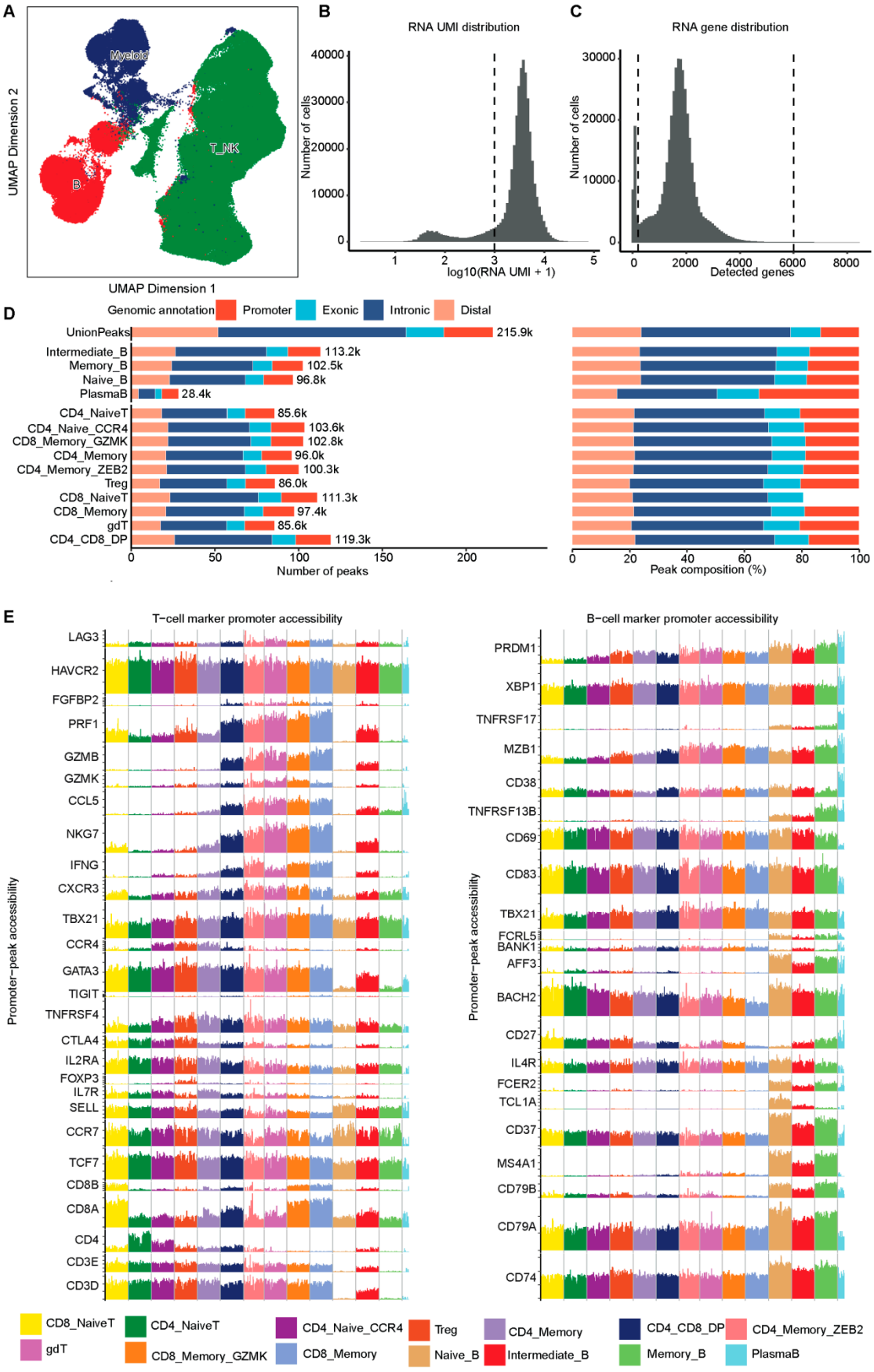


Figure S1. Quality control and characterization of single-nucleus multi-omic profiles of adaptive immune cells following COVID-19 vaccination

(A) UMAP visualization of T cells and B cells subsets.

(B) Distribution of RNA UMI counts across cells.

(C) Distribution of the number of detected genes across cells.

(D) Bar plot showing the genomic annotation of called ATAC-seq peaks across different genomic regions.

(E) Genome browser tracks showing chromatin accessibility and called peaks at representative marker genes.

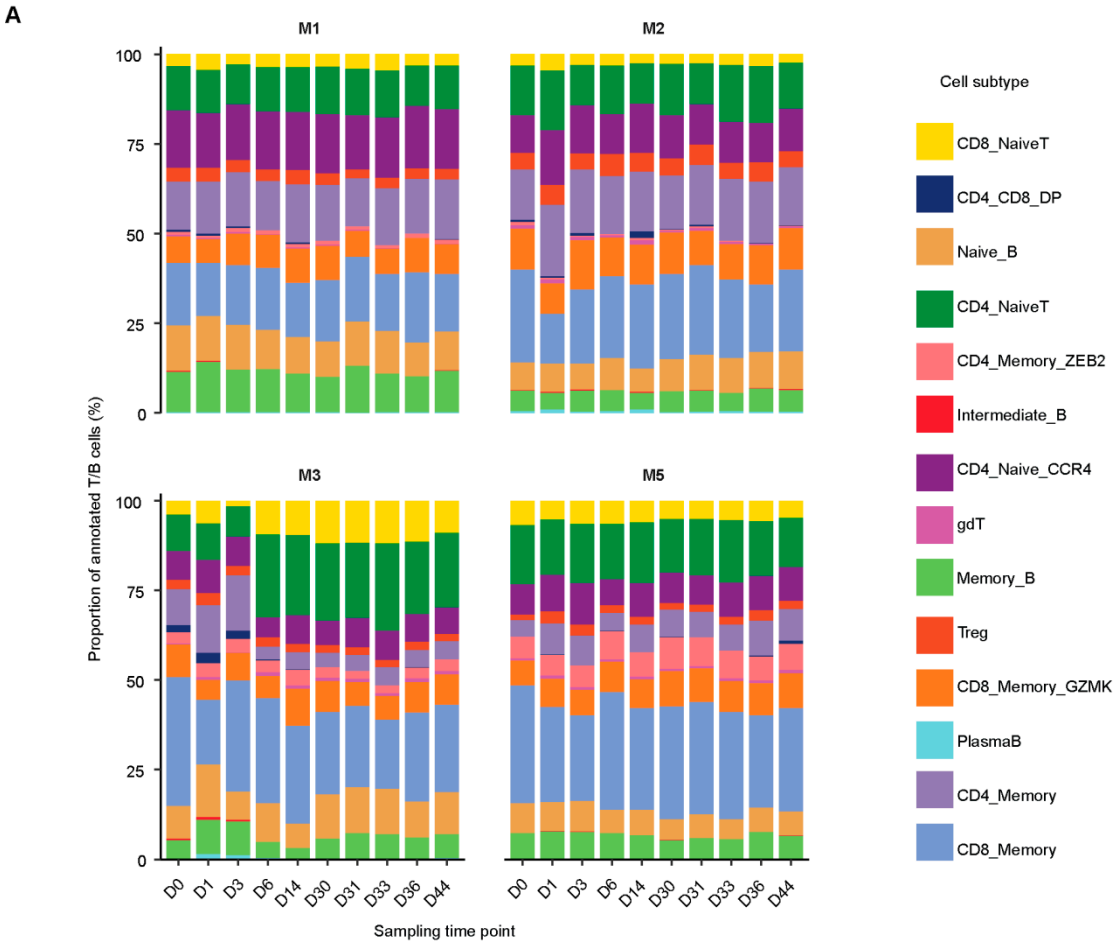


Figure S2. Stacked bar plots showing cell-subset composition at each time point, displayed separately for each donor.

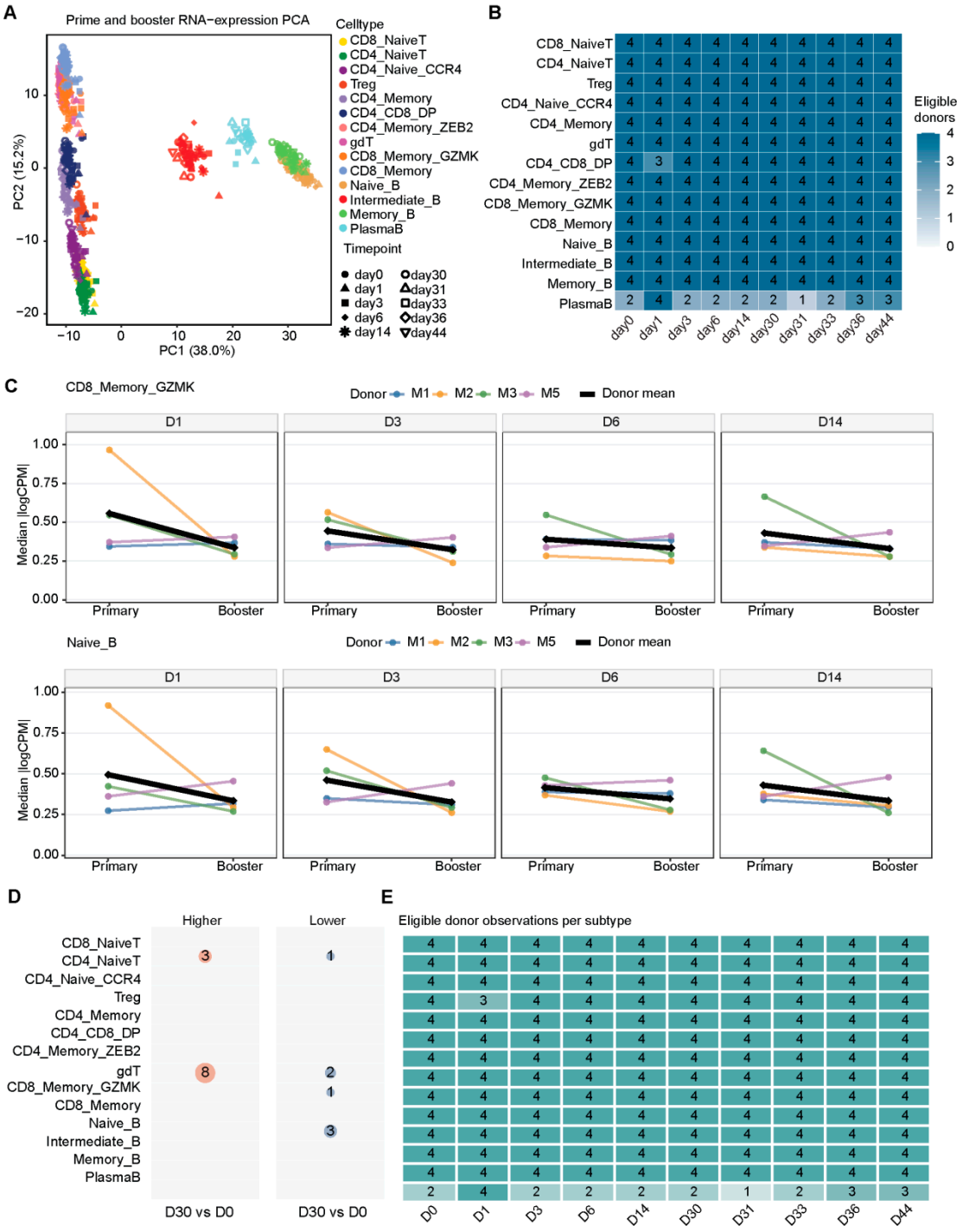

A
Prime and booster RNA−expression PCA
PC2 (15.2%)
PC1 (38.0%)
Celltype
CD8_NaiveT
CD4_NaiveT
CD4_Naive_CCR4
Treg
CD4_Memory
CD4_CD8_DP
CD4_Memory_ZEB2
gdT
CD8_Memory_GZMK
CD8_Memory
Naive_B
Intermediate_B
Memory_B
PlasmaB
Timepoint
day0 day30
day1 day31
day3 day33
day6 day36
day14 day44
B
Eligible donors
day0 day1 day3 day6 day14 day30 day31 day33 day36 day44
C
CD8_Memory_GZMK
Donor M1 M2 M3 M5 Donor mean
D1 D3 D6 D14
Median |logCPM|
Primary Booster
Naive_B
D
Higher
Lower
D30 vs D0
E
Eligible donor observations per subtype

Figure S3. Dynamic transcriptomic of T- and B-cell subsets following prime and booster vaccination.

(A) Principal component analysis (PCA) of pseudobulk RNA expression profiles across the longitudinal sampling series. Each point represents a cell subtype at a given time point. Colors indicate immune cell subtypes, and point shapes indicate sampling time points.

(B) Heatmap showing the number of eligible donors for each cell-subset–time-point combination. Numbers indicate donor counts, and color intensity represents coverage from zero to four donors. Eligibility required at least 10 cells per donor-time-point-subset combination.

(C) Paired comparisons of response magnitudes after primary and booster vaccination in CD8 Memmory_GZMK and Naive B cells at matched post-vaccination intervals of 1, 3, 6, and 14 days. Each point represents one donor, and connecting lines link observations from the same donor. Each comparison included donors with eligible observations at all four relevant time points. Thick lines connect the mean response magnitudes across the paired donors.

(D) Numbers of upregulated and downregulated genes at D30 relative to D0, identified by donor-adjusted edgeR quasi-likelihood analysis of raw-count pseudobulk profiles, using BH FDR ≤ 0.10 and $|\log_2 FC| \geq 0.50$.

(E) Numbers of eligible donors at each time point and in each cell subset; eligibility required at least 10 cells per donor-time point-subset combination.

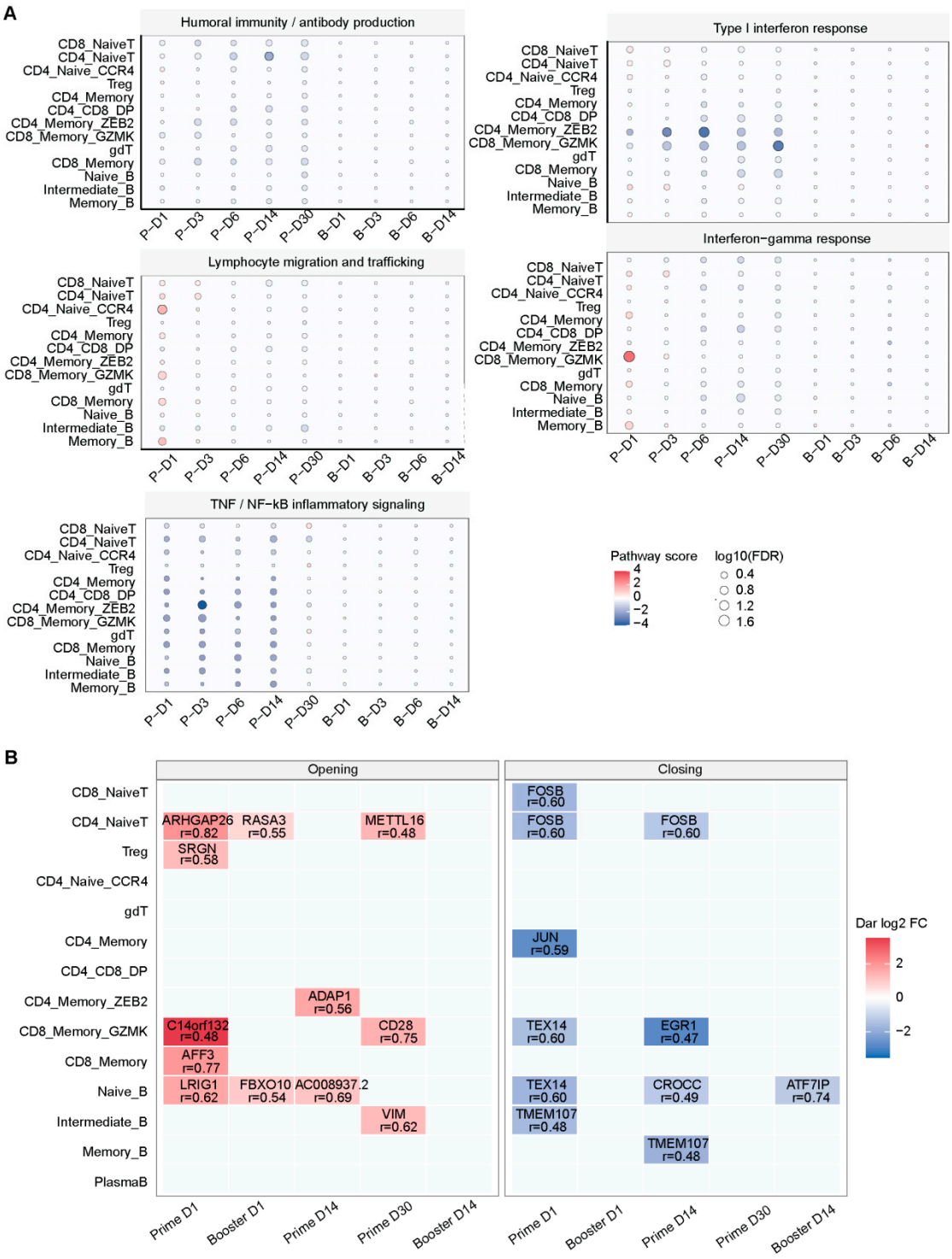


Figure S4. Dynamic chromatin-accessibility remodeling of T- and B-cell subsets following prime and booster vaccination.

(A) Dynamic enrichment of humoral immunity, lymphocyte migration and trafficking, TNF/NF-κB inflammatory pathways, type I interferon response and interferon gamma response pathways across immune cell subtypes. Dot color indicates the pathway score, with red and blue representing positive and negative scores, respectively, and

dot size represents statistical significance as -log10(FDR).

(B) Heatmap showing log2 fold changes in the expression of genes linked to differentially accessible regions (DARs).

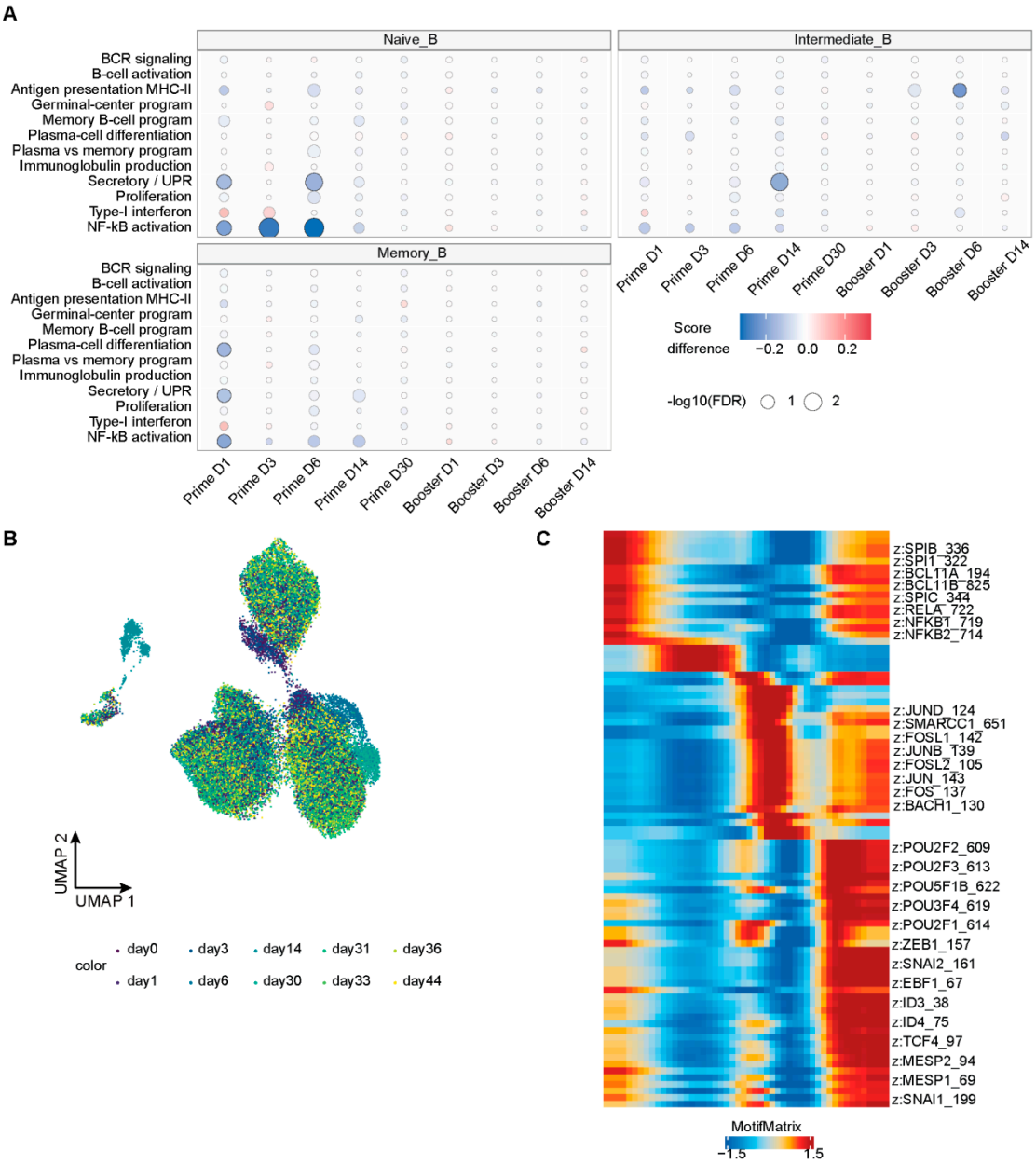


Figure S5. Functional and trajectory-associated chromatin remodeling of B-cell subsets following vaccination.

(A) Dot plot showing functional modules scores across B cells, including B cell receptor signal transduction, B cell activation, MHC II antigen presentation, germinal center activity, memory B cell identity, plasma cell differentiation, plasma cell polarization and memory cell polarization, immunoglobulin production, secretory and unfolded protein response, proliferation, type I interferon response, and NF-κB activation. Dot color indicates the average module score of each B cell subset.

(B) UMAP visualization of B cells subsets across timepoints.

(C) Heatmap showing chromVAR TF motif deviation scores the B cell trajectory.

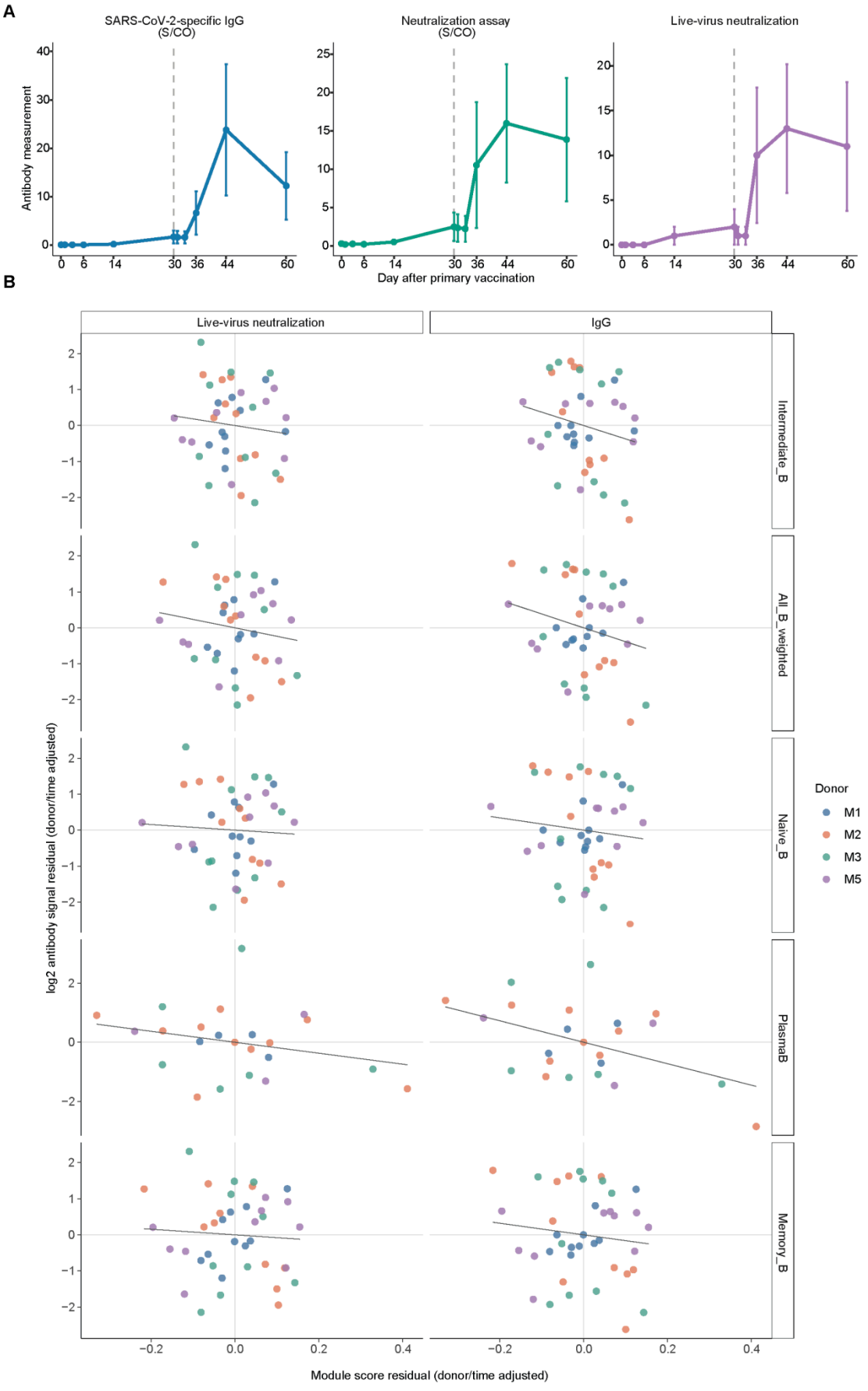

A
SARS-CoV-2-specific IgG (S/CO)
Neutralization assay (S/CO)
Live-virus neutralization
Antibody measurement
Day after primary vaccination
B
Live-virus neutralization
IgG
Intermediate_B
All_B_weighted
Naive_B
PlasmaB
Memory_B
log2 antibody signal residual (donor/time adjusted)
Module score residual (donor/time adjusted)
Donor
M1
M2
M3
M5

Figure S6. Longitudinal serum antibody measurements and exploratory associations with B-cell Secretor module scores following BBIBP-CorV vaccination.

(A) SARS-CoV-2-specific IgG, competitive-inhibition antibody measurements, and live-virus neutralization titers across time points. Points and lines represent means, and error bars indicate SEM across four participants. The dashed vertical line marks the second dose at D30. Serological data were previously reported in our group's companion study of the same cohort.

(B) Associations between existing Secretory/UPR module scores and matched antibody measurements in individual B-cell subsets and the cell-count-weighted aggregate B-cell population. Each point represents one donor-time-point observation, colored by donor.

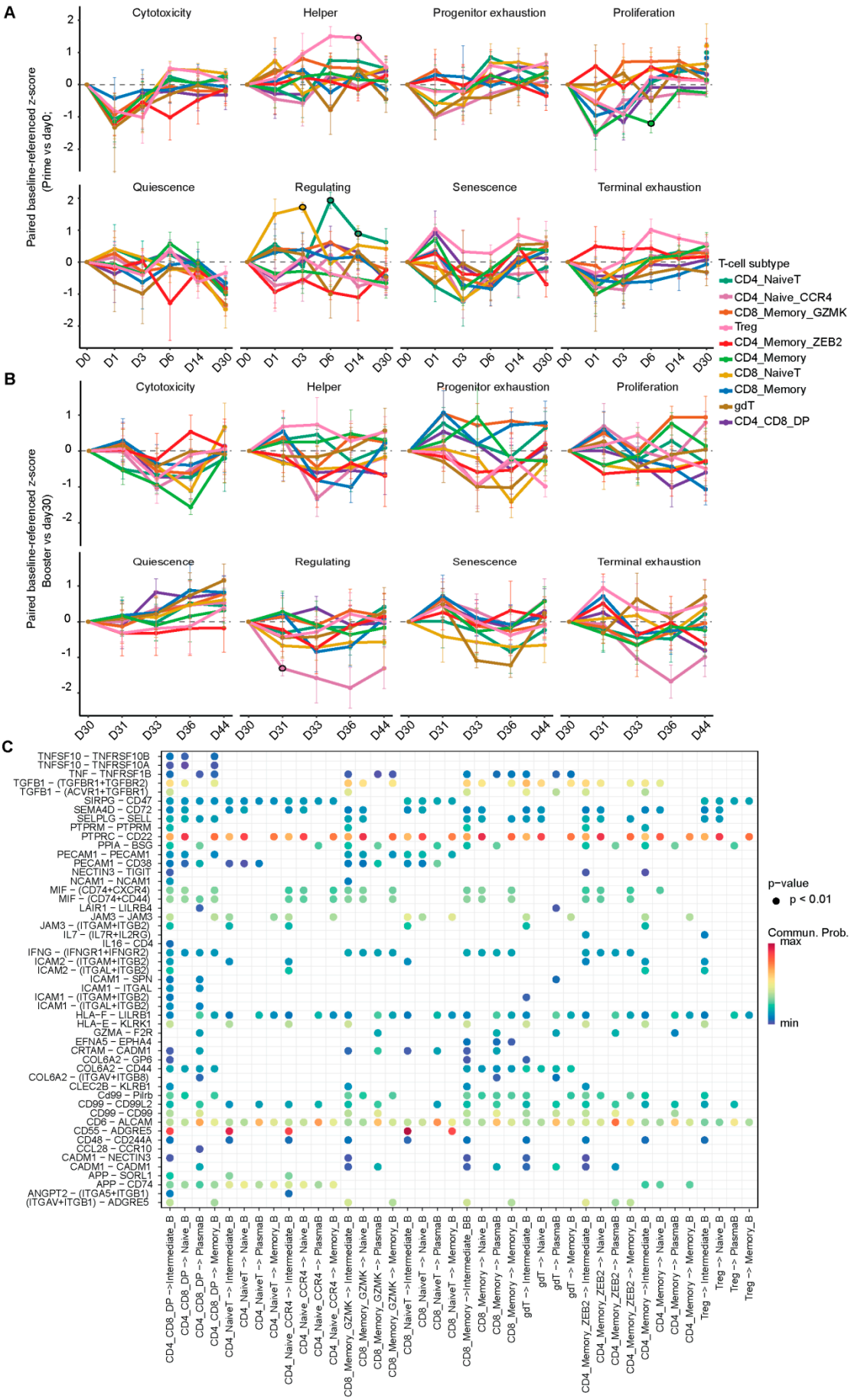

A
Cytotoxicity
Helper
Progenitor exhaustion
Proliferation
Quiescence
Regulating
Senescence
Terminal exhaustion
Paired baseline-referenced z-score
(Prime vs day0;
D0
D1
D3
D6
D14
D30
B
Paired baseline-referenced z-score
Booster vs day30)
D30
D31
D33
D36
D44
T-cell subtype
CD4_NaiveT
CD4_Naive_CCR4
CD8_Memory_GZMK
Treg
CD4_Memory_ZEB2
CD4_Memory
CD8_NaiveT
CD8_Memory
gdT
CD4_CD8_DP
C
TNFSF10 – TNFRSF10B
TNFSF10 – TNFRSF10A
TNF – TNFRSF1B
TGFB1 – (TGFBR1+TGFBR2)
TGFB1 – (ACVR1+TGFBR1)
SIRPG – CD47
SEMA4D – CD72
SELPLG – SELL
PTPRM – PTPRM
PTPRC – CD22
PPIA – BSG
PECAM1 – PECAM1
PECAM1 – CD38
NECTIN3 – TIGIT
NCAM1 – NCAM1
MIF – (CD74+CXCR4)
MIF – (CD74+CD44)
LAIR1 – LILRB4
JAM3 – JAM3
JAM3 – (ITGAM+ITGB2)
IL7 – (IL7R+IL2RG)
IL16 – CD4
IFNG – (IFNGR1+IFNGR2)
ICAM2 – (ITGAM+ITGB2)
ICAM2 – (ITGAL+ITGB2)
ICAM1 – SPN
ICAM1 – ITGAL
ICAM1 – (ITGAM+ITGB2)
ICAM1 – (ITGAL+ITGB2)
HLA-F – LILRB1
HLA-E – KLRK1
GZMA – F2R
EFNA5 – EPHA4
CRTAM – CADM1
COL6A2 – GP6
COL6A2 – CD44
COL6A2 – (ITGAV+ITGB8)
CLEC2B – KLRB1
Cd99 – Plirb
CD99 – CD99L2
CD99 – CD99
CD6 – ALCAM
CD55 – ADGRE5
CD48 – CD244A
CCL28 – CCR10
CADM1 – NECTIN3
CADM1 – CADM1
APP – SORL1
APP – CD74
ANGPT2 – (ITGA5+ITGB1)
(ITGAV+ITGB1) – ADGRE5
CD4_CD8_DP ->Intermediate_B
CD4_CD8_DP -> Naive_B
CD4_CD8_DP -> PlasmaB
CD4_CD8_DP -> Memory_B
CD4_NaiveT -> Intermediate_B
CD4_NaiveT -> Naive_B
CD4_NaiveT -> PlasmaB
CD4_NaiveT -> Memory_B
CD4_Naive_CCR4 -> Intermediate_B
CD4_Naive_CCR4 -> Naive_B
CD4_Naive_CCR4 -> PlasmaB
CD4_Naive_CCR4 -> Memory_B
CD8_Memory_GZMK -> Intermediate_B
CD8_Memory_GZMK -> Naive_B
CD8_Memory_GZMK -> PlasmaB
CD8_Memory_GZMK -> Memory_B
CD8_NaiveT ->Intermediate_B
CD8_NaiveT -> Naive_B
CD8_NaiveT -> PlasmaB
CD8_NaiveT -> Memory_B
CD8_Memory ->Intermediate_BB
CD8_Memory -> Naive_B
CD8_Memory -> PlasmaB
CD8_Memory -> Memory_B
gdT ->Intermediate_B
gdT -> Naive_B
gdT -> PlasmaB
gdT -> Memory_B
CD4_Memory_ZEB2 -> Intermediate_B
CD4_Memory_ZEB2 -> Naive_B
CD4_Memory_ZEB2 -> PlasmaB
CD4_Memory_ZEB2 -> Memory_B
CD4_Memory ->Intermediate_B
CD4_Memory -> Naive_B
CD4_Memory -> PlasmaB
CD4_Memory -> Memory_B
Treg ->Intermediate_B
Treg -> Naive_B
Treg -> PlasmaB
Treg -> Memory_B
p-value
p < 0.01
Commun. Prob.
max
min

Figure S7. Functional remodeling of T-cell subsets and dynamic T-B-cell communication following primary vaccination.

(A) Line graph showing the longitudinal T-cell status scores across ten T-cell subtypes relative to day 0 after primary vaccination. Colored lines and dots represent the average scores for each T-cell subtype. The black circles indicate significant differences.

(B) Line graph showing the longitudinal T-cell status scores across ten T-cell subtypes relative to day 30 after booster vaccination. Colored lines and dots represent the average scores for each T-cell subtype. The black circles indicate significant differences.

(C) Significant ligand-receptor interactions between T cells and B cells. Only interactions with statistically significant communication probability (adjusted $P < 0.05$) are shown. Dot size represents communication probability, and color intensity indicates interaction strength.

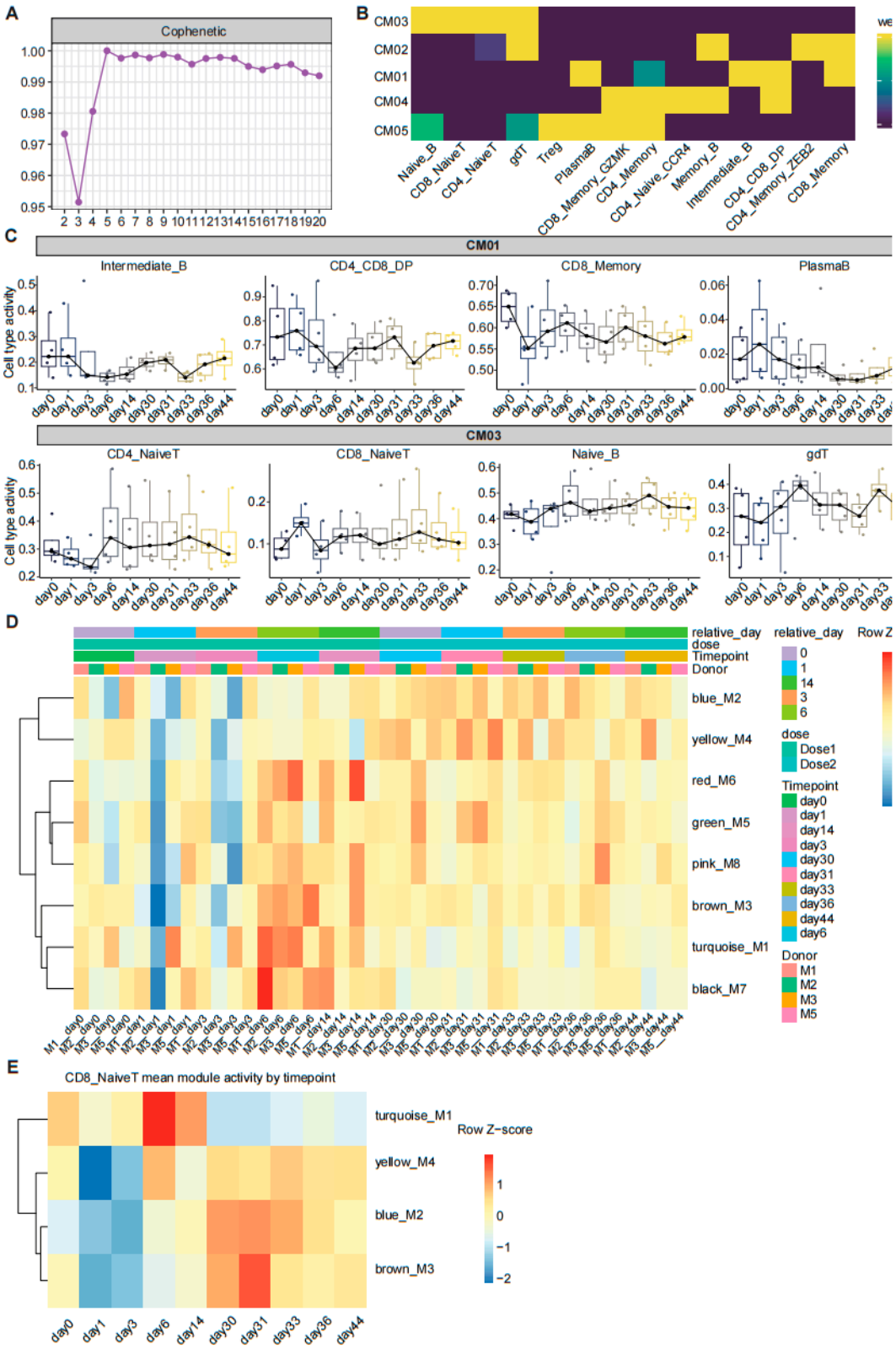


Figure S8. Temporal organization and transcriptional features of cross timepoint cellular modules following primary and booster vaccination.

(A) NMF rank selection based on cophenetic correlation and consensus stability, with rank 5 selected for downstream analysis.

(B) Heatmap showing the weights of each cell type in the CM.

(C) Line graph showing the changes in the abundance of four representative cell subsets associated with CM01 and CM03 across the vaccination series.

(D) Heatmap showing normalized gene expression of WGCNA gene modules across ten time points in Intermediate B cells.

(E) Heatmap showing the normalized gene expression of WGCNA gene modules across ten time points in CD8 naive T cells.